ELSEVIER

Chemical Engineering Journal 80 (2000) 237–244

Chemical Engineering Journal

www.elsevier.com/locate/cej

Crossflow filtration testing of INEEL radioactive and non-radioactive waste slurries

N.R. Mann*, T.A. Todd

Lockheed Martin Idaho Technologies Company, Idaho National Engineering and Environmental Laboratory, PO Box 1625, Idaho Falls, ID 83415-5218, USA

Abstract

Development of waste treatment processes for the remediation of radioactive wastes is currently under way at the Idaho Nuclear Technology and Engineering Center (INTEC), located at the Idaho National Engineering and Environmental Laboratory (INEEL). INTEC, formerly known as the Idaho Chemical Processing Plant, previously reprocessed nuclear fuel to retrieve fissionable uranium. Liquid waste raffinates resulting from reprocessing were solidified into a calcine material. Waste treatment processes currently being considered include the dissolution of the solidified calcine material and separation of residual undissolved solids (UDS). UDS in solution must be removed prior to downstream processes such as solvent extraction and ion exchange. Filtration experiments were conducted at the INEEL using a crossflow filter apparatus on radioactive and non-radioactive waste slurries [N.R. Mann, T.A. Todd, Evaluation and Testing of the Cells Units Crossflow Filter on INEEL Dissolved Calcine Slurries, INEEL/EXT-98-00749, Idaho National Engineering and Environmental Laboratory, Idaho Falls, ID, 1998]. The purpose of this testing was to evaluate the removal and operational efficiency of crossflow filtration on slurries of various solids loadings. The solids loadings tested were 0.19, 2.44 and 7.94 wt.%, respectively. A matrix of test patterns was used to determine the effects of transmembrane pressure and axial velocity on filtrate flux. Filtrate flux rates for each solids loading displayed a high dependence on transmembrane pressure, indicating that pressure filtration resistance limits filtrate flux. Filtrate flux rates for all solids loading displayed a negative dependency on axial velocity. This would suggest axial velocities tested were efficient at removing filter cake. Prior to testing of actual waste slurries, baseline water runs were performed. Filtrate flowrates observed during baseline water runs exhibited substantial decreases despite numerous backpulses and rinses, suggesting particles that were deeply embedded within the filter membrane as the result of shear-induced deagglomeration

Keywords: Solid–liquid separation; Filtration; Crossflow; Radioactive waste slurries; Idaho National Engineering and Environmental Laboratory

1. Introduction

Development of waste stream processes for the remediation of radioactive wastes is currently under way at the Idaho Nuclear Technology and Engineering Center (INTEC). INTEC, formerly known as the Idaho Chemical Processing Plant, previously reprocessed nuclear fuel to retrieve fissionable uranium. Solids formed from precipitation and absorption of radioactive ions require separation from the liquid phase to prevent bed fouling and downstream contamination prior to solvent extraction and/or ion exchange processes.

The purpose of this filter study was to evaluate crossflow filtration as effective solid–liquid separation technology for treating Idaho National Engineering and Environmental Laboratory (INEEL) waste slurries, outline operating conditions and examine filter flowrates.

1.1. Crossflow filtration technology

Crossflow filtration operates differently than traditional filtration methods. Crossflow filtration operates by recirculating the feed flow parallel to the filter membrane. The velocity of the suspension in recirculation sweeps away particles concentrated on the filter membrane, thereby limiting the thickness of filter cake. Permeate flows perpendicular to the feed stream rather than parallel to the feed stream. Traditional filtration methods such as dead-end filtration operate with feed flow and permeate flow in the same direction. Dead-end filtration creates a concentration of particles (filter cake) on the filter membrane [1]. Fig. 1 displays the comparison between traditional dead-end filtration and crossflow filtration.

1.2. Theory

With all forms of filtration, the greatest hindrance to liquid flow through the filter membrane is particle accumulation

* Corresponding author. Tel.: +1-208-5268644; fax: +1-208-5263499.
E-mail address: mannnr@inel.gov (N.R. Mann).

1383-5866/00/$ – see front matter
PII: S1383-5866(00)00096-4

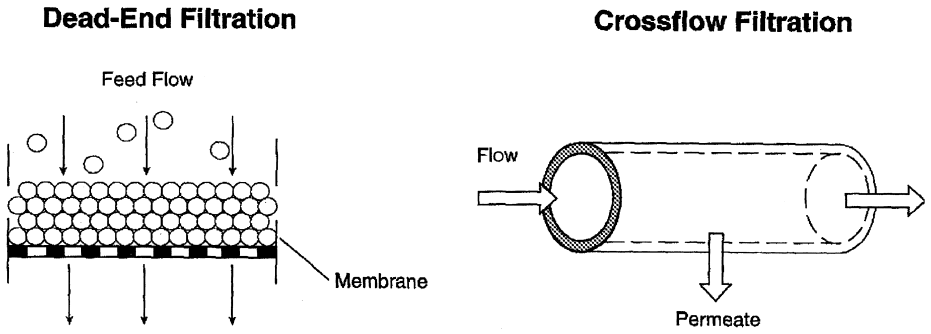

Fig. 1. Comparison of traditional dead-end filtration with crossflow filtration.

(filter cake). By utilizing a high-fluid circulation rate parallel to the filter membrane, the accumulation of particles on the filter surface can be minimized. Although crossflow filtration minimizes this accumulation, it does not eliminate it.

Several mechanisms are present in a crossflow filtration system, which affect filtrate flow. An excellent discussion by Geeting and Reynolds explains the theory surrounding two mechanisms known as mass transport resistance and pressure filtration resistance, which are the two primary resistances to filtrate flux [2].

Back transport of solids away from the membrane and the bulk stream is required to prevent the cake thickness from continually increasing. Both a filter cake and boundary layer may be present in a crossflow filtration system. A schematic representation of crossflow filtration showing the filter membrane, the filter cake, the boundary layer and the bulk stream is shown in Fig. 2.

If the limiting resistance to filtrate flux is due to the back transport of solids away from the membrane, then

$$J_{mt} = k \ln\left(\frac{C_w}{C_b}\right) \tag{1}$$

where, J_{mt}, mass transfer limited flux; k, back mass transfer coefficient; C_w, concentration at the wall; C_b, concentration in the bulk stream.

If mass transport does not limit filtrate flow, then filtrate flux should vary in accordance with Darcy's equation for pressure filtration.

$$J_f = \frac{P}{\mu}\left(\frac{L}{K} + R_m\right) \tag{2}$$

where, J_f, pressure filtration limited flux (m^3/m^2 S); P, filtration pressure (Pa); μ, liquid viscosity (Pa S); R_m, filter media resistance (1/m); L/K, filter cake resistance; where, L, cake thickness (m) and K, cake permeability (m^2).

Eq. (2) indicates the filtration rate J_f increases when P increases; K increases, or μ decreases. The filtration rate J_f decreases when L increases, and R_m increases.

Two operational regimes exist for crossflow filtration. In the first regime, the filtrate flux is a function of pressure. In the second regime, it is not. These two regimes are described as follows.

1.2.1. Regime I

Suppose a given system at steady state with set axial velocity and constant filtration flux, J_{mt} as described by Eq. (1). If the filtration flux described by Eq. (1) is greater than that described by Eq. (2) (i.e. $J_{mt} > J_f$), then the filtrate flux will vary linearly with pressure because the flux will be limited as described by Darcy's filtration equation (Eq. (2)). On the other hand, for the same system at set pressure with $J_{mt} > J_f$, an increase in velocity may or may not increase flux. An increase in axial velocity will not result in higher filtrate flux unless it causes the resistance to decrease (thus increasing

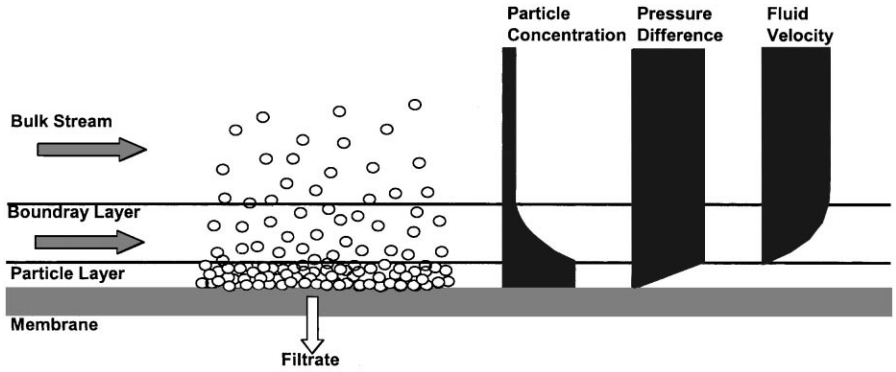

Fig. 2. Schematic representation of crossflow filtration.

J_f). If the given axial velocity is effective at keeping the filter cake resistance low, axial velocity will not significantly affect the filtrate flux.

1.2.2. Regime II

Given the same system described, with conditions such that $J_{mt}=J_f$. In this regime, the flux will no longer vary with pressure. Increased pressure will bring about an increase in cake resistance, R_c, (L/K) by means of growth in cake thickness or decrease in the cake permeability (or both). While an increase in pressure may cause $J_{mt}<J_f$ temporarily, velocity alone is effective in increasing the filtrate flux.

From Eq. (1) we see that increased solid in the feed, C_b, causes J_{mt} to decrease. Therefore, increasing solids loading decreases the pressure at which $J_{mt}=J_f$; and a given system can switch from regime I to regime II merely by increasing the solids loading in the feed.

1.3. Crossflow filtration apparatus

Although numerous solid–liquid separation technologies are commercially available, few are adaptable to high radiation fields. The crossflow filtration apparatus was fabricated for operation within a shielded cell. The apparatus consists mainly of stainless steel Swagelok fittings, valves and gauges. One 0.5 μm, 0.480-in. i.d., 6-in. length Mott sintered Hastelloy filter element was used in the test. A Moyno progressive cavity pump provided slurry feed solution, which is contained, within the slurry reservoir. Slurry temperature is measured by a type-J thermocouple installed in a thermowell within the slurry reservoir. A schematic of the crossflow filtration apparatus is shown in Fig. 3 [3].

Three sets of tests were performed with the crossflow filtration apparatus. Each set consisted of a series of 13 experimental test conditions. Prior to each condition, two separate backpulses were performed at 45 and 70 psig. Backpulses were conducted by opening the V-3 backpulse valve, filling the backpulse chamber. The chamber is pressurized by opening the three-way V-7 backpulse valve until the predetermined pressure is attained. The V-7 valve is then closed and the V-3 valve is opened, allowing the pressurized filtrate to backpulse the filter.

At the completion of the second backpulse, a timer was started. Filtrate flowrates were measured by means of a fill-and-drain-graduated cylinder. Filtrate flowrate measurements were taken in 5-min increments for a span of 30 min. Axial velocity, transmembrane pressure, filtrate flux and temperature data were also recorded in addition to filtrate flow. Transmembrane pressure and axial velocity were controlled by adjusting the pump speed and the throttle valve (V-1).

2. Experimental

2.1. Test conditions

Three sets of tests were performed with the crossflow filtration apparatus, each consisting of a series of 13 experimental test conditions. A two-parameter central composite

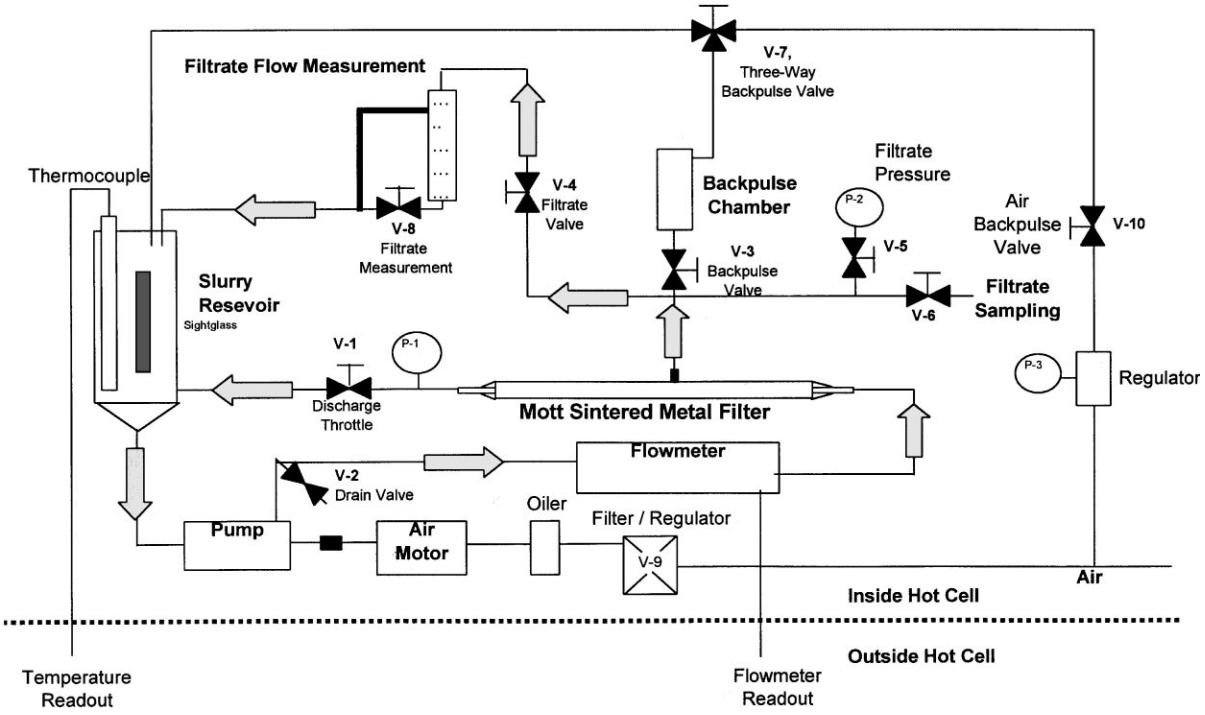

Fig. 3. Schematic of the CUF apparatus.

Table 1
Conditions and run order used in testing of the crossflow filtration apparatus

Condition	Axial velocity (ft/s)	Transmembrane pressure (psig)
1	6.0	20.0
2	7.5	27.5
3	3.0	20.0
4	6.0	5.0
5	7.5	12.5
6	6.0	20.0
7	4.5	27.5
8	6.0	35.0
9	4.5	12.5
10	9.0	20.0
11	6.0	20.0
12	6.0	45.0
13	6.0	55.0

design, which varied transmembrane pressure from 5 to 55 psig and axial velocity from 3 to 9 ft/s, was used to determine the effects of transmembrane pressure and axial velocity on filtrate flux [2].

Table 1 displays the various conditions and run order used in testing at the INEEL. The center condition (1, 6 and 11) was tested three times for the purpose of repeatability. Testing of the center condition assisted in the determination of filter fouling at a similar axial velocity and transmembrane pressure at various stages during the test (first, middle and last).

2.2. Baseline water run conditions

Baseline water runs were performed prior to the testing of actual and simulated waste slurries. Baseline water runs assisted in the determination of filter fouling between actual waste slurries. Approximately 800 ml of deionized water, free from any solids, was utilized for individual water runs. Nine test conditions were performed in succession, excluding conditions 6 and 11, which are analogous to condition 1. Preceding each water run, the filter membrane was extensively rinsed (including several backpulses) with deionized water until no solids were collected from the rinse solution. The nine experimental baseline water run test conditions are shown in Table 2.

Table 2
Nine experimental baseline water run test conditions

Condition	Axial velocity (ft/s)	Transmembrane pressure (psig)
1, 6, 11	6.0	20.0
2	7.5	27.5
3	3.0	20.0
4	6.0	5.0
5	7.5	12.5
7	4.5	27.5
8	6.0	35.0
9	4.5	12.5
10	9.0	20.0

2.3. Feed solutions

Two slurry feed solutions were utilized in the testing of the crossflow filtration apparatus. The first test was performed 831 ml of actual radioactive waste slurry containing 0.19 wt.% solids loading. The second test was performed using the same radioactive waste slurry with additional undissolved solids (UDS). To increase solids loading, an additional 23.06 g were added to the previous solution. The combined concentration of UDS in solution was 2.44 wt.%. The third and final test was performed using approximately 800 ml of non-radioactive waste slurry containing 7.94 wt.% solid loading.

3. Results and discussion

3.1. Baseline water run results

The filtrate flowrate (ml/s) for each of the nine conditions performed is shown in Fig. 4. The filtrate flowrate (ml/s) is plotted against the nine test conditions. Relatively, high filtrate flowrates were observed for water run 1. This was expected, due to the installation of a new Mott sintered Hastelloy filter prior to testing. Higher filtrate flowrates can be observed at higher transmembrane pressures, such as conditions 2, 7 and 8. Lower filtrate flowrates are observed in conditions with a lower transmembrane pressure. These results confirm the Hagen–Poiseuille equation, which accurately predicts clean water flux through cylindrical pores [5].

$$\eta = \pi r^2 \Delta \frac{pt}{8VL} \tag{3}$$

where, η, shear viscosity; π, 3.1415926; Δp, pressure drop; t, time it takes for a volume, V of liquid to flow through a capillary of length, L; r, pore radius.

The equation states that liquid flux is proportional to the transmembrane pressure and inversely proportional to the liquid viscosity, which is controlled by the solute concentration and the temperature. Therefore, increasing the pressure or the temperature results in an increase in flux [5].

Filtrate flowrate values for baseline water runs 2, 3 and 4 are substantially lower, compared with flowrates shown in water run 1. Backpulsing was unsuccessful at restoring the filtrate flowrate to the original values shown in water run 1. It is apparent that particles within the pores of the filter membrane were not removed, despite extensive rinsing and backpulsing.

3.2. Radioactive waste slurry (0.19 wt.%)

Fig. 5 displays the filtrate flux (gpm/ft^2) for conditions 1–13 as a function of time (min) since backpulse. Filtrate flux was calculated by dividing the volumetric filtrate flowrate by the filter area. A substantial decrease in flux is observed through the first 5 min, after which the rate of decline lessens substantially. Steady state is achieved

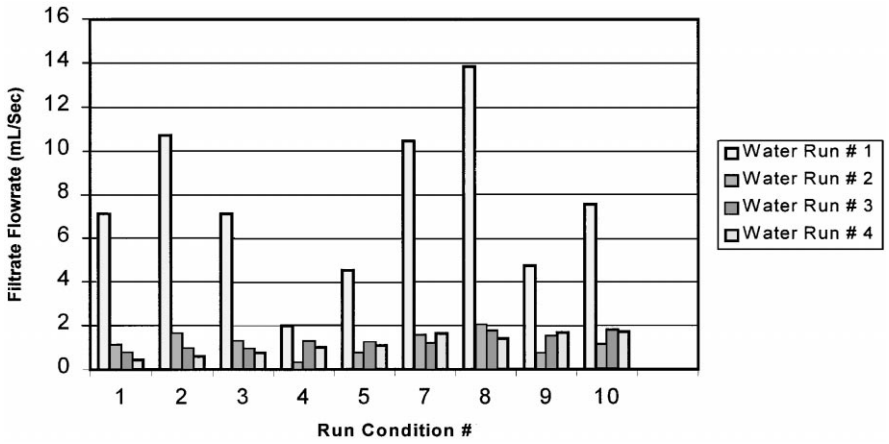

Fig. 4. Filtrate flowrate (ml/s) for each of the ten conditions tested.

at approximately 25 min after backpulse. Backpulses prior to each condition appear to restore filtrate flux, however, considerable filter fouling is observed within 5 min after backpulse. The rate of filter cake accumulation is slightly less than the rates observed at higher solids loadings. At 20 min from backpulse, an increase in flux is observed for conditions 4 and 13. A theory, which might explain the random increase in flux, is the accumulation and dispersion of particles on the needle valve (V-1).

Fig. 6 displays the filtrate flux as a function of time (min) since backpulses for conditions 1, 6 and 11, all tested at 6 ft/s axial velocity and 20 psig transmembrane pressure. Filtrate flux values appear to be very similar, despite a slight variance in initial flux. Filtrate flux values for conditions 6 and 11 are shown slightly higher than condition 1 at time zero. This would suggest inconsistent backpulse techniques. This theory is confirmed by the union of all three conditions at 5 min after backpulse.

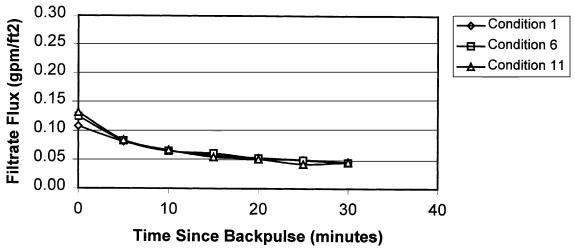

Fig. 6. Filtrate flux as a function of time since backpulse for conditions 1, 6 and 11, at 0.19 wt.% solids loading.

3.3. Radioactive waste slurry (2.44 wt.%)

Fig. 7 displays the filtrate flux (gpm/ft^2) for conditions 1–13 as a function of time (min) since backpulse. A distinct decrease in flux is observed through the first 5 min, after which the rate of decrease lessens. Steady state is achieved at approximately 20 min since backpulse. Backpulsing prior to each condition appears to restore filtrate flux, however flux quickly diminishes. Steady state is achieved sooner than with the lower solids loading of 0.19 wt.%. This would indicate that the formation of the filter cake is achieved much sooner compared with lower solids loadings.

Fig. 8 displays the filtrate flux as a function of time (min) since backpulse for conditions 1, 6 and 11, all tested at 6 ft/s axial velocity and 20 psig transmembrane pressure. Filtrate

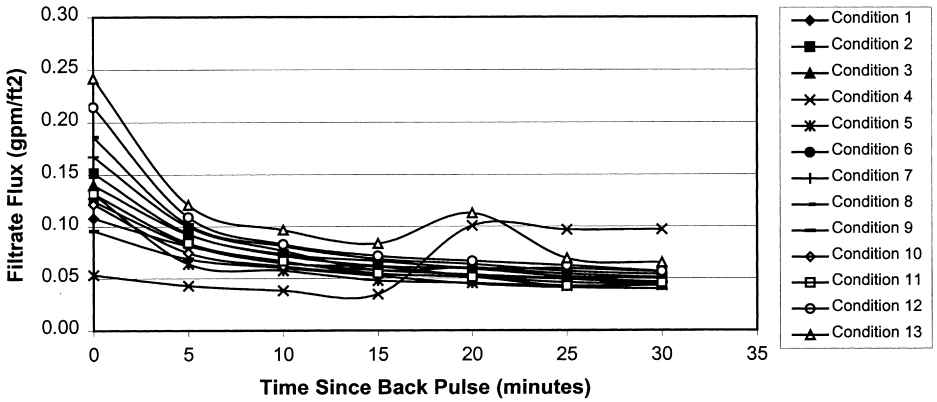

Fig. 5. Filtrate flux as a function of time since backpulse for conditions 1–13 at 0.19 wt.% solids loading.

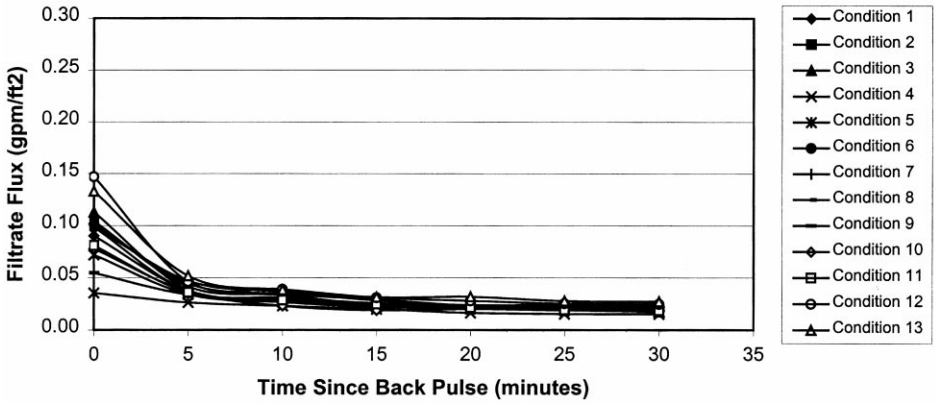

Fig. 7. Filtrate flux as a function of time since backpulse for conditions 1–13 at 2.44 wt.% solids loading.

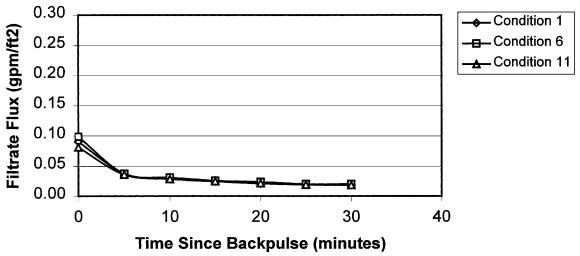

Fig. 8. Filtrate flux as a function of time since backpulse for conditions 1, 6 and 11, at 2.44 wt.% solids loading.

flux values appear to be very similar, despite a slight variance in initial flux. Similar variations were observed in testing at 0.19 wt.%. Filtrate flux values for condition 6 are slightly higher than condition 1 at time zero. This would suggest inconsistent backpulse techniques. This theory is confirmed by the union of all three conditions at approximately 5 min since backpulse.

3.4. Non-radioactive waste slurry (7.94 wt.%)

Fig. 9 displays the filtrate flux (gpm/ft^2) for conditions 1–13 as a function of time (min) since backpulse. A substantial decrease in flux is observed through the first 5 min, after which a steady state is achieved. Steady state is achieved sooner than with the previous tests at lower solids loading. This would indicate that formation of filter cake is achieved sooner compared with lower solids loading. Backpulsing prior to each condition appears to restore filtrate flux; however, severe filter fouling is evident after 5 min since backpulse.

Fig. 10 displays filtrate flux as a function of time (min) since backpulse for conditions 1, 6 and 11, all tested at 6 ft/s axial velocity and 20 psig. Filtrate flux rates for conditions 6 and 11 are shown slightly higher than condition 1 at time zero. This would suggest inconsistent backpulse techniques. This theory is confirmed by the union of all three conditions at 5 min since backpulse. Similar variations observed during testing of 0.19 and 2.44 wt.% solids loading imply inconsistent backpulse techniques performed for all tests. Despite variations of filtrate flux, backpulses appear to restore filter performance. Nevertheless, increased filtrate flux could be achieved by optimizing backpulse techniques.

3.5. Filtrate flux comparison

Fig. 11 displays the filtrate flux as a function of transmembrane pressure for 0.19, 2.44 and 7.94 wt.% solids

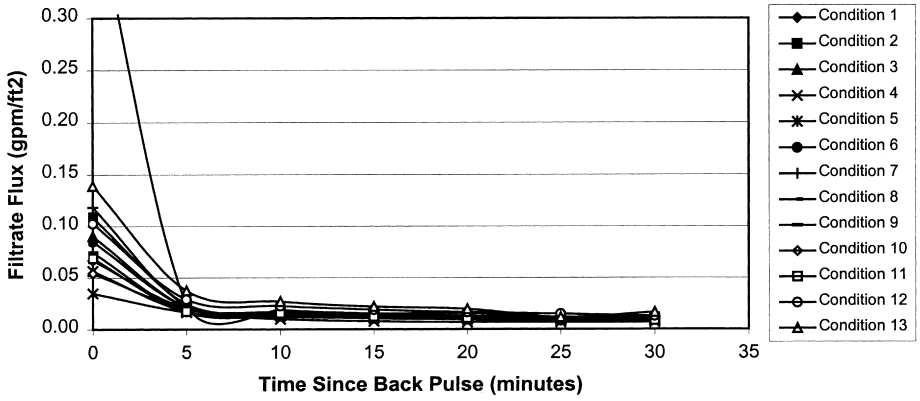

Fig. 9. Filtrate flux as a function of time since backpulse for conditions 1–13 at 7.94 wt.% solids loading.

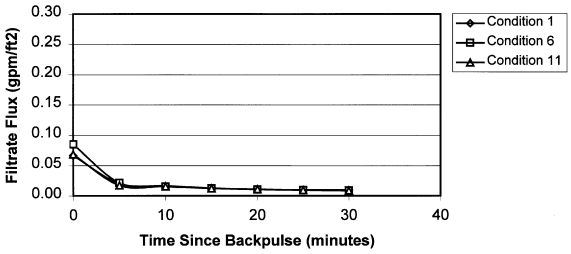

Fig. 10. Filtrate flux as a function of time since backpulse for conditions 1, 6 and 11, at 7.94 wt.% solids loading.

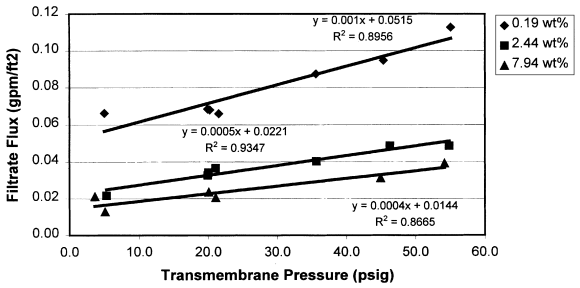

Fig. 11. Filtrate flux as a function of transmembrane pressure for 0.19, 2.44 and 7.94 wt.% solids loading.

loading, respectively. The filtrate flux dependence on transmembrane pressure is approximately linear for all solids loadings, specifying the operating regime as regime I. A decrease of both slope and filtrate flux are observed with the increased solids loading. A gradual decrease of transmembrane pressure dependence can be observed with increased solids loading. These data suggest a gradual transition from regime I to regime II. From Eq. (1), increased solids in the feed, C_b causes J_{mt} to decrease. Therefore, increasing solids loading decreases the pressure at which $J_{mt}=J_f$ and a given system can switch from regime I to regime II by simply increasing solids loading in the feed [2]. Additional increases in solids loading would incite the critical value at which the filtrate flux loses its dependence on pressure.

Fig. 12 displays filtrate flux as a function of axial velocity for 0.19, 2.44 and 7.94 wt.% solids loading, respectively. Decreases in slope and filtrate flux are observed with increased solids loading. Axial velocities are sufficient for removing filter cake, despite operating in regime I. Additional increases in axial velocity will not increase filtrate flux. The operating system, at the highest solids loading, suggests the system is approaching regime II.

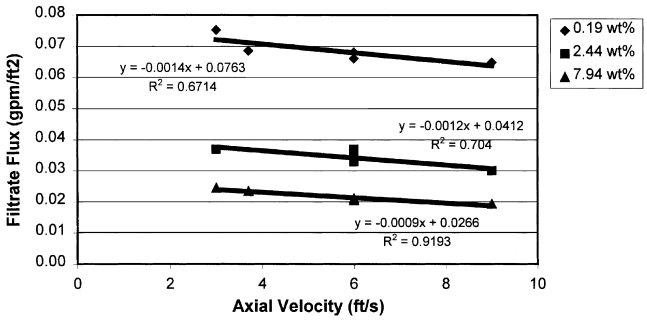

Fig. 12. Filtrate flux as a function of axial velocity for 0.19, 2.44 and 7.94 wt.% solids loading.

Table 3
Filter efficiencies for 2.44 and 7.94 wt.% solids loading

Sample	H-4 (2.44 wt.%)	1027 (7.94 wt.%)
Tare weight (filter unit)	68.160 (g)	56.532 (g)
Gross weight (UDS and filter unit)	68.214 (g)	56.547 (g)
Remaining UDS	0.054 (g)	0.015 (g)
Reduction in solids loading	99.139%	99.925%

Filtrate flux rates observed were substantially lower than expected. This decrease possibly suggests particles deeply embedded within the filter membrane. One theory proposed by Peterson and Nash [4], that could possibly explain decreases in filtrate flow, describes the formation of a filter cake within the pores of the filter (and extending to barely cover the surface of the filter) [4]. A similar phenomenon observed by Murkes and Carlsson [6] describes a decrease in flux due to internal plugging of the pores [6]. Additional data displaying a substantial decrease in filtrate flow during baseline water run 2 confirm this theory. Shear deagglomeration is believed to be the main cause of filter fouling. Shear deagglomeration decreases particle size, which can induce internal plugging and/or lessen filter cake permeability. Moreover, if such a filter cake exists, increases in axial velocity would neither affect the cake and/or filtrate flux, since the filter cake would not be exposed to the bulk slurry.

3.6. Filter efficiency

Two, 200-ml effluent samples were collected to determination filter efficiency. Samples were taken by way of the V-6 filtrate-sampling valve. Filtrate samples were filtered through a Cole–Parmer 500 ml, 0.45 μm filter unit and weighed. The remaining weight was used to determine filter efficiency. One sample was collected utilizing actual radioactive waste slurry containing 2.44 wt.% solids loading. The second 200-ml sample was collected utilizing the non-radioactive waste slurry containing 7.94 wt.% solids loading. Each sample was obtained following two backpulses at the completion of condition 13. Filter efficiency calculations using the 2.44 and 7.94 wt.% solids loadings filtrate effluents are shown in Table 3.

4. Summary

The evaluation of crossflow filtration for the removal of UDS present in radioactive and non-radioactive waste slurries is presented in the following conclusions.

- Solids loading in radioactive waste slurry containing 2.44 wt.% solids displayed a 99.139% reduction in solids loading.
- Solids loading in non-radioactive waste slurry containing 7.94 wt.% solids displayed a 99.925% reduction in solids loading.
- Filtrate flux rates for all solids loadings displayed high dependencies for transmembrane pressures indicating filtrate flux is controlled by Darcy's equation. Moreover, filtrate flux rates for all solids loadings displayed negative dependencies for axial velocity, suggesting that all axial velocities tested were effective at removing filter cake.
- Backpulsing proved to be beneficial at restoring filtrate flux, however, initial baseline filtrate flux rates were not achieved. Shear induced deagglomeration is believed to be the main cause of filter fouling.
- Filtrate flux rates observed at time zero, displayed variations for recurrent conditions 1, 6 and 11. This would indicate backpulse procedures performed during test were inconsistent.
- Crossflow filtration was effective at filtering 0.19, 2.44 and 7.94 wt.% solids loading and is a viable method for the removal of UDS from INEEL radioactive and non-radioactive waste slurries.

Acknowledgements

This work was supported by the US Department of Energy, Office of Science and Technology's Tanks Focus Area.

References

[1] US Department of Energy, Office of Science and Technology, Innovative Technology Summary Report #350, 'Crossflow Filtration' February 1998.
[2] J.G.H. Geeting, B.A. Reynolds, Bench–Scale Crossflow Filtration of Tank S-107 Sludge Slurries and Tank C-107 Supernatant, PNNL-11376 (UC-721), Pacific Northwest National Laboratory, Richland, WA, 1996.
[3] J.L. Tripp, E.L. Wade, FY-97 Experimental Results of the Cells Unit Crossflow Filter Tests at the INEEL, INEEL/EXT-97-01232, Idaho National Engineering and Environmental Laboratory, Idaho Falls, ID, 1997.
[4] R.A. Peterson, C.A. Nash, Filter Performance Mechanisms (U), WSRC-TR-95-0420, Westinghouse Savannah River Company, Aiken, SC, 1995.
[5] D. Brose, M. Dosmar, S. Cates, F. Hutchison, Studies on the scale-up of crossflow filtration devices, PDA J. Pharm. Sci. Technol. 50 (4) (1996).
[6] J. Murkes, C.G. Carlsson, Crossflow Filtration, Wiley, New York, NY, 1988.